

Maxillary Sinus Floor Augmentation with Two Different Inorganic Bovine Bone Grafts: an Experimental Study in Rabbits

Vitor FERREIRA BALAN¹, Daniele BOTTICELLI², David PEÑARROCHA-OLTRA³, Katsuhiko MASUDA⁴, Eduardo PIRES GODOY¹, Samuel Porfirio XAVIER¹

Objective: To compare the sequential healing of maxillary sinuses grafted with two different xenogeneic bone substitutes processed at either a low (300°C) or high (1200°C) temperature.

Methods: A sinus augmentation procedure was performed bilaterally in 20 rabbits and two different xenogeneic bone grafts were randomly used to fill the elevated spaces. Healing was studied after 2 and 10 weeks, in 10 rabbits during each period.

Results: After 2 weeks of healing, very small amounts of new bone were observed in both groups, and were mainly confined to close to the sinus bone walls and osteotomy edges. After 10 weeks of healing, new bone was found in all regions, with higher percentages in those close to the bone walls and to the osteotomy. In this period of healing, the proportion of new bone in the 300°C group was 20.0% ± 4.3%, and in the 1200°C group it was 17.2% ± 4.3% ($P = 0.162$). In the 1200°C group, translucent, dark fog-like shadows in regions of the grafts were hiding portions of new bone (interpenetrating bone network).

Conclusion: Both biomaterials provided conditions that allowed bone growth within the elevated space, confirming that both biomaterials are suitable to be used as a graft for sinus floor augmentation.

Key words: animal study, bone healing, histology, sinus floor augmentation, sinus membrane
Chin J Dent Res 2022;25(2):93–105; doi: 10.3290/j.cjdr.b3086337

Maxillary sinus augmentation is a widely used procedure to restore the bone volume lost in the posterior maxilla in patients who require implant-supported rehabilitation¹.

Several studies have shown that the sinus mucosa tends to return to its original position if implants or

biomaterials are not inserted into the space created by its elevation^{2,3}. To counteract the volume shrinkage, the use of biomaterials⁴, implants⁵⁻⁹ or devices¹⁰⁻¹³ has been suggested. Autogenous bone is still considered the filler of choice for sinus floor augmentation¹⁴; however, high rates of volumetric resorption of autogenous bone have been reported^{15,16}, in addition to the surgical morbidity associated with the donor bed¹⁷. Several grafting materials have been used to fill the augmented maxillary sinus, among which xenogeneic bone granules, derived from different animal species, have been studied in the literature⁴. Among the xenogeneic graft materials, a deproteinised bovine bone mineral (DBBM) processed at a low temperature (300°C) has been used in several clinical¹⁸⁻²³ and animal studies^{2,3,15,24-26}. This xenogeneic bone presents slow resorption and excellent osteoconductive properties^{24,27-29}. Another deproteinised bovine bone produced only from the pure mineral bovine bone phase and sintered at a high temperature

1 Department of Oral and Maxillofacial Surgery and Periodontology, University of São Paulo, Faculty of Dentistry of Ribeirão Preto, São Paulo, Brazil.

2 ARDEC Academy, Rimini, Italy.

3 Department of Stomatology, Faculty of Medicine and Dentistry, University of Valencia, Valencia, Spain.

4 Department of Paediatric Dentistry, Division of Oral Infection and Disease Control, Osaka University, Osaka, Japan.

Corresponding author: Dr Daniele Botticelli, ARDEC Academy, Viale Giovanni Pascoli 67, Rimini, Italy. Tel: 39-0541393444. Email: daniele.botticelli@gmail.com

The study was supported by ARDEC Academy, Rimini, Italy. The Cerabone material was provided free of charge by Straumann Italy.

(> 1200°C) has been used for sinus floor augmentation³⁰⁻³⁵. This xenogeneic graft has also been employed in animal experiments, using different models and sites such as chambers prepared in skinfolds on the back of hamsters³⁶, critical defects in the rabbit ulna³⁷, circumferential defects around dental implants in minipigs³⁸ or critical-size calvarium defects in albino rats³⁹. An animal model using rabbits for maxillary sinus augmentation surgery has been shown to be the most appropriate for experiments, mainly due to its similarity to the human anatomy; both have wide and accessible cavity, well-defined ostium and a mucociliary system with the same characteristics^{40,41}.

A comparative clinical study of Bio-Oss (Geistlich, Wolhusen, Switzerland) and Cerabone (Botiss Biomaterials, Zossen, Germany) used in maxillary sinus augmentation surgery found that Cerabone had larger particles (1:2.7) and a less intense gradual release of calcium ions³⁰. Moreover, in a radiographic evaluation conducted after 4 years, a more pronounced volumetric loss was observed for Bio-Oss compared to Cerabone³⁰. An *in vitro* study reported a higher level of hydrophilicity for Cerabone compared to Bio-Oss⁴².

In histological analyses, maxillary sinuses of rabbits filled with DBBM presented a good amount of newly formed bone, providing maintenance of the space created within the elevated area^{2,3,24}. There are no reports in the literature involving maxillary sinus augmentation in animals that compared the results of healing using Bio-Oss and Cerabone as fillers. Thus, the aim of the present study was to compare the sequential healing of maxillary sinuses grafted with two different xenogeneic bone substitutes processed at either a low or high temperature.

Materials and methods

Ethical statements

The experimental protocol was approved by the Ethical Committee of the Faculty of Dentistry of Ribeirão Preto, University of São Paulo, São Paulo, Brazil on 8 April 2019 (protocol #2019.1.113.58.1). The article was written according to the Animal Research: Reporting of In Vivo Experiments (ARRIVE) guidelines. The Brazilian rules for animal care were followed strictly.

Animal sample

A total of 20 adult male New Zealand white rabbits weighing approximately 3.5 to 4.0 kg and aged 5 to 6 months were used in the present study following a previously published methodology⁴³.

Study design and sample calculation

A randomised split-mouth design was used to eliminate interferences between subjects in the same group. Sinus augmentation was performed bilaterally and two different bovine xenogeneic bone materials, sintered at 300°C (Bio-Oss group) or 1200°C (Cerabone group), were used to fill the two augmented spaces. Two healing periods were analysed, namely 2 and 10 weeks, with 10 animals each period.

The sample size was determined considering data from a previous study available at the time of sample size calculation²⁸, applying $\alpha = 0.05$, power = 0.8 and a correlation between measures of 0.5. Thus, for this configuration, the sample size was 10 animals per group (two groups, $n = 10$) to enable the authors to find statistical significance between the experimental groups.

Biomaterials

Bio-Oss is a DBBM with sinterisation at 300°, porosity of 75% to 80%, pores of 20 to 200 μm and a mean particle size of 0.5 to 1.0 mm^{44} . Cerabone, meanwhile, is formed completely by hydroxyapatite from bovine cancellous bone, with sinterisation at 1200°C, porosity of 65% to 80%, pores of 600 to 900 μm and a mean particle size of 0.5 to 1.0 mm^{44} .

Randomisation and allocation concealment

Randomisation between groups and periods of healing was performed electronically (randomization.com) by an author who was not involved in the selection and handling of animals and/or surgical procedures (SPX) on 5 May 2019. The treatment allocations were secured in opaque sealed envelopes and revealed to the surgeon (VFB) immediately after completion of the osteotomy and sinus mucosa elevation.

Surgical procedures

The surgical procedures were performed by one expert surgeon (VFB), preceded by injection of acepromazine maleate (1.0 mg/kg; Acepran, Vetnil, Louveira, SP, Brazil), xylazine (3.0 mg/kg; Dopaser, Hertape Calier, Juatuba, MG, Brazil) and ketamine hydrochloride (50 mg/kg; Ketamin Agener, União Química Farmacêutica Nacional, Embu-Guaçú, São Paulo, Brazil). Through an incision in the nasal dorsum, the nasal bone was exposed, and osteotomies were created bilaterally to the naso-incisal suture (Fig 1a). The sinus mucosa was elevated and the subnasal spaces were randomly filled

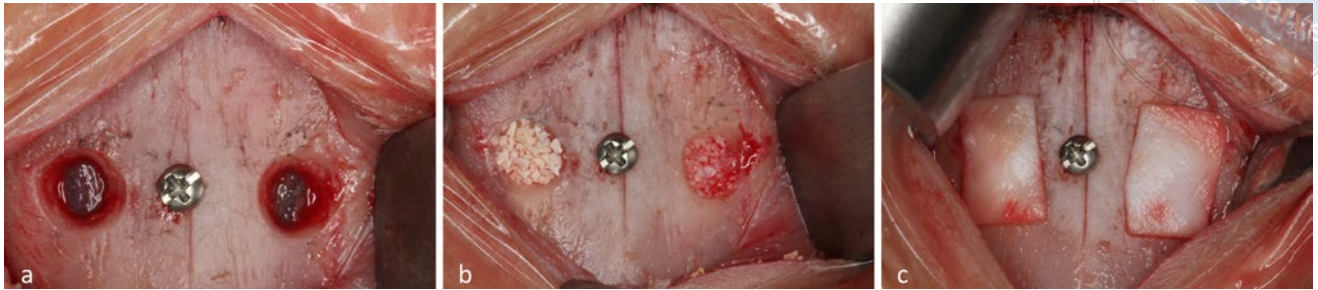


Fig 1 Clinical view of the nasal dorsum and the two osteotomies lateral to the naso-incisal suture. **(a)** Both osteotomies prepared; a small screw was placed in the naso-incisal suture between the centres of the osteotomies to assist the subsequent histological processing; **(b)** xenogeneic bone grafts placed within the elevated space: Cerabone on the left and Bio-Oss on the right; **(c)** collagen membranes placed on the osteotomies.

with similar amounts of the two biomaterials (Fig 1b). The osteotomies were subsequently covered using a collagen membrane (Bio-Gide, Geistlich; Fig 1c), and the wounds were closed with sutures.

Maintenance care

The animals were housed in individual cages placed in climatized rooms with access to food and water ad libitum. The biological functions and the wounds were monitored by veterinarians over the whole period of the experiment.

Euthanasia

The rabbits were first anaesthetised following similar procedure exposed above and then euthanised in a closed transparent acrylic box containing gas carbon dioxide (CO₂). The region of interest was harvested and fixed in 10% formaldehyde.

Microcomputed tomography (microCT) evaluations

A 1172 microcomputed tomography (microCT) system (Bruker, Kontich, Belgium) was used to take microCT scans of the specimens. The parameters used were 9.92 µm isotropic pixel, 60 KV/165, 134 µA, filter Al 0.5 mm, exposure time 596 ms, rotation step 0.4 degrees, frame average 4, and random movement 10. The analyses were performed using DataViewer (Bruker).

Histological preparation

Precision cutting/grinding equipment (Exakt, Apparatebau, Norderstedt, Germany) was used to prepare two histological slides from each biopsy specimen after

dehydration, inclusion in resin (LR White Hard Grid, London Resin, Berkshire, UK) and polymerisation. The small screw placed in the naso-incisal suture was used as a reference. The two slides were stained with either toluidine blue or Stevenel's blue and alizarin red.

Histometric evaluations

Photomicrographs were taken under the microscope (Leica DMLB, Wetzlar, Germany) using a digital camera (Digital Sight DS-2Mv, Nikon, Tokyo, Japan).

The following regions were analysed within the elevated space (Fig 2): medial bone wall (M), lateral bone wall (L), sub-sinus region (S), central area (C) and osteotomy region (A).

A grid of 80 squares was superimposed on the images of the histological slides using the software Image J 1.50i (National Institutes of Health, Bethesda, MD, USA) and a point-counting procedure at 100× magnification was adopted for morphometric measurements⁴⁵. New bone (not covered by graft shadows), interpenetrating bone network (IBN; see-through bone graft in the Cerabone group) and residual xenogeneic bone were assessed. Total bone was calculated as the sum of new bone and IBN. Percentages were calculated with respect to the total area of the region evaluated and a mean value was obtained for the five regions. Before taking the measurements, calibration with another expert examiner (SPX) was performed until an inter-class correlation coefficient $k > 0.9$ was achieved for tissue recognition.

Data analysis

The primary variable was the mean total bone percentage in the full elevated space. The data from the various

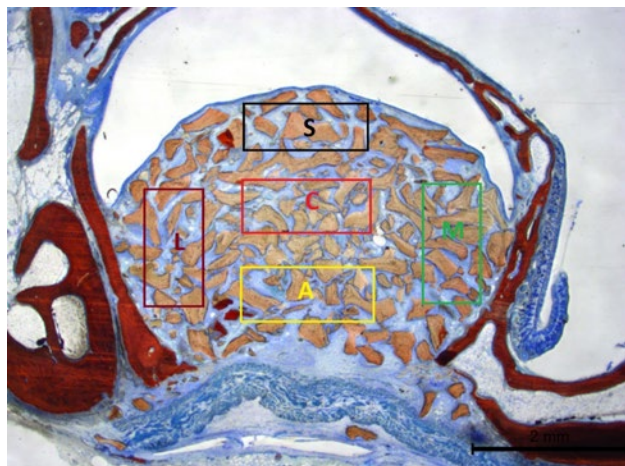


Fig 2 References scheme. Five regions of the sinus were identified: the osteotomy region (A), the central area of the graft (C), the sub-sinus region, subjacent to the sinus mucosa (S), and the regions close to the medial (M) and lateral bone walls (L).

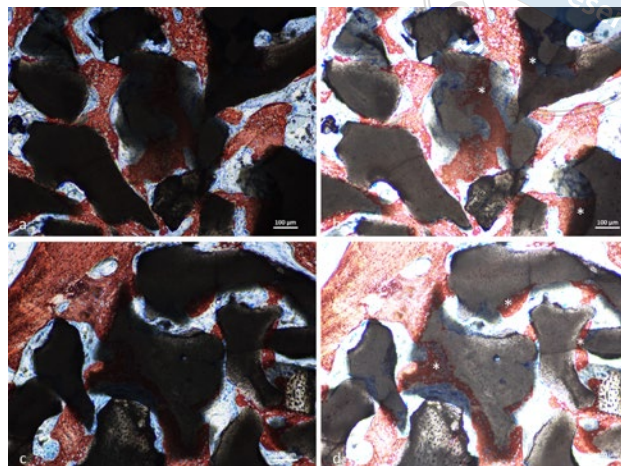


Fig 3 Photomicrographs of ground sections of Cerabone sites after 10 weeks of healing. Note the translucent dark fog-like shadow regions that, after increasing the light intensity, revealed new bone (IBN). **(a and c)** Normal light intensity; **(b and d)** high light intensity. The white asterisks indicate examples of IBN regions.

regions were used to establish a more detailed description of bone formation.

Prism 9.1.1 (GraphPad Software, San Diego, CA, USA) was used for statistical analyses. The normal distribution of the variables was assessed with a Shapiro-Wilk test for both paired and unpaired variables. Either a paired *t* test or a Wilcoxon test was used to evaluate the differences between the Bio-Oss and Cerabone groups. Differences between the two healing periods were evaluated using either an unpaired *t* test or a Mann-Whitney test.

A Spearman two-tailed correlation coefficient was applied to measure the strength of the correlation between the outcomes of the histological and microCT analyses. GraphPad Prism 9.1.1 was used. The correlation coefficient and *P* values were reported. *P* < 0.05 was considered statistically significant.

The tables listed mean values, standard deviations, *P* values, medians and 25% and 75% percentiles, whereas in the text only mean values were reported.

Results

Descriptive histological evaluation

In the histological analysis, the surface of the biomaterial was well defined for the Bio-Oss granules whereas for Cerabone, translucent dark fog-like shadows gave

the granules an undefined periphery. In some instances, especially at the 10-week period, these shadows hid the presence of new bone that was unveiled when light intensity was increased when the photomicrographs were taken under the microscope (IBN; Figs 3a to d). After 2 weeks of healing, very small amounts of new bone were observed in both groups, mainly confined to close to the sinus bone walls and osteotomy edges, whereas the other regions were practically devoid of new bone (Figs 4a and b). The graft material occupied almost half of the elevated space.

Ridges of new bone sprouting from the sinus bone walls towards the centre of the elevated space incorporated the nearest granules in both the Cerabone (Fig 5a) and Bio-Oss (Fig 5b) groups. The granules furthest from the bone walls were instead surrounded by soft tissue, presenting a dense layer of fibroblast-like cells disposed along the graft surface. Some osteoclast-like cells were also seen on the surface of both biomaterials (Figs 5a and b). The osteotomy was still covered by the collagen membrane (Figs 4a and b) involved in degradation processes. New bone was forming from the edges of the osteotomies, aiming to close the defect (Figs 5c and d). A few granules were found in some specimens beyond the osteotomy in both groups.

After 10 weeks of healing, new bone was found in all regions, with higher percentages recorded in regions close to the bone walls and the osteotomy (Figs 6a and b). The granules presented a higher grade



Fig 4 Photomicrographs of ground sections after 2 weeks of healing. **(a)** Cerabone site; **(b)** Bio-Oss site. Stevenel's blue and alizarin red staining were used. The yellow arrows indicate new bone forming from the mesial bone walls of the sinus on both sides.

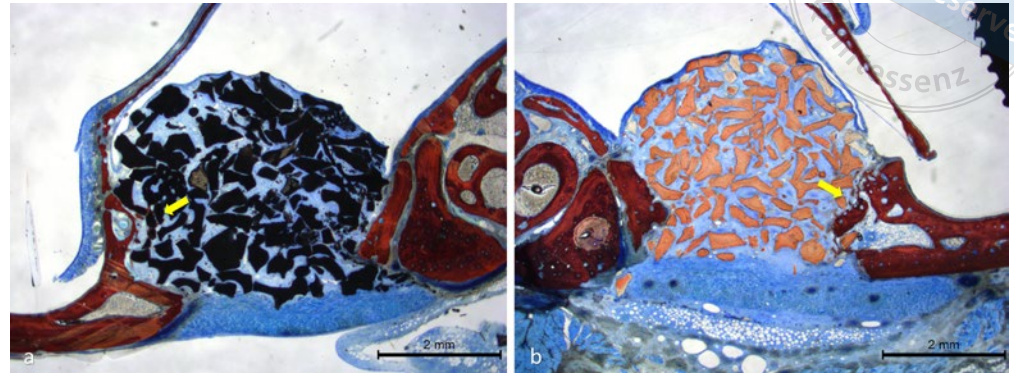


Fig 5 Photomicrographs of ground sections after 2 weeks of healing. New bone formed from the bone walls surrounded the closest **(a)** Cerabone and **(b)** Bio-Oss granules. New bone forming from the osteotomy edge at the **(c)** Cerabone and **(d)** Bio-Oss sites. **(a and b)** Stevenel's blue and alizarin red staining; **(c and d)** toluidine blue staining. The yellow arrows indicate new bone, the yellow asterisks mark old parent bone, the red asterisks show biomaterial and the red arrows indicate osteoclasts.

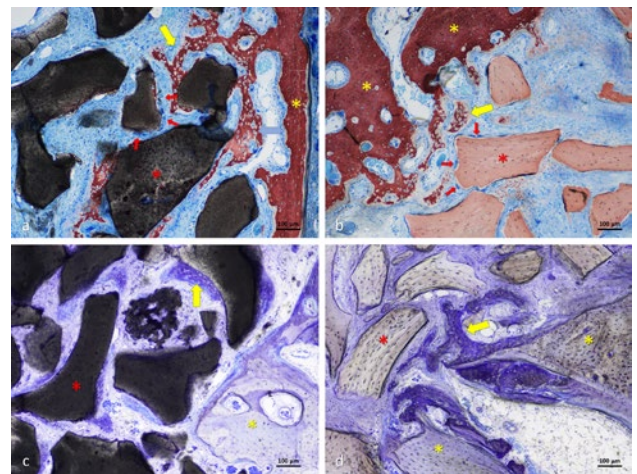
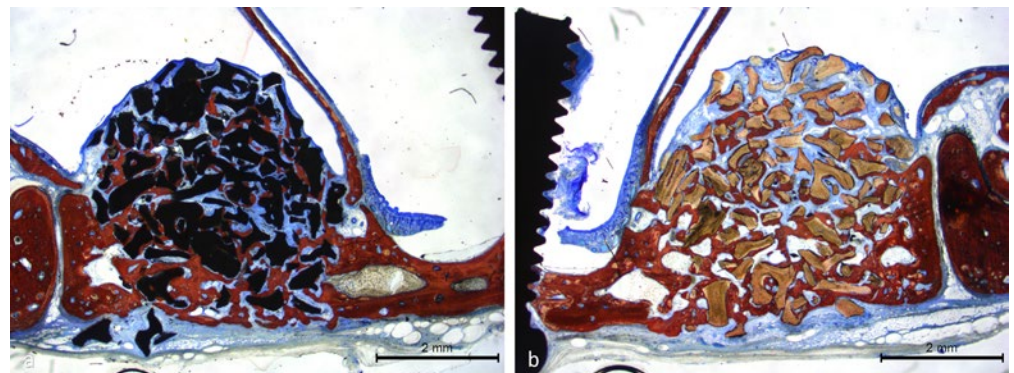


Fig 6 Photomicrographs of ground sections after 10 weeks of healing. New bone was found in all regions examined at both **(a)** Cerabone and **(b)** Bio-Oss sites. Stevenel's blue and alizarin red staining were used.



of incorporation into newly formed bone compared to the previous healing period (Figs 7a and d). The regions subjacent to the sinus mucosa presented the lowest amounts of new bone. Most of the osteotomies were closed by newly formed bone with signs of remodelling. The degradation of the collagen membrane was not completed yet (Figs 6a and b). Some granules were found beyond the osteotomy and several perforations of the sinus mucosa were observed for both biomaterials.

Histometric evaluation

After 2 weeks of healing (Table 1), IBN was almost absent such that both new bone and total bone fractions were 0.7% and 0.3% for the Bio-Oss and Cerabone groups, respectively ($P = 0.098$). The residual graft fraction was 43.4% for the Bio-Oss group and 48.8% for the Cerabone group ($P = 0.037$).

New bone was mostly located close to the sinus bone walls (Table 2). A slight tendency towards higher bone

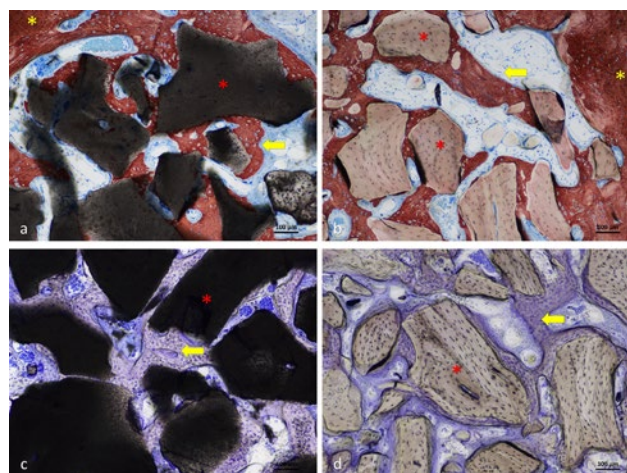


Fig 7 Photomicrographs of ground sections after 10 weeks of healing. New bone incorporated the granules of both biomaterials and formed bridges that interconnected the granules. **(a and c)** Cerabone and **(b and d)** Bio-Oss granules. **(a and b)** Stevenel's blue and alizarin red staining; **(c and d)** toluidine blue staining.

formation was seen in the Bio-Oss group compared to the Cerabone group in all regions. The submucosa region was virtually devoid of new bone in both groups. None of the differences between groups were statistically significant considering the various regions.

After 10 weeks of healing (Table 1), small fractions of IBN were found in the Cerabone group (1.3%). Total bone was found in proportions of 20.0% in the Bio-Oss group, and 17.2% in the Cerabone group ($P = 0.162$).

The residual graft decreased with respect to the previous healing period to 36.4% and 35.3% ($P = 0.846$) in the Bio-Oss and Cerabone groups, respectively (Fig 8). In both groups, the differences between periods in total bone and residual graft percentages were statistically significant ($P < 0.05$).

In both groups, the regions presenting the greatest amount of new bone were those close to the window, followed by those close to the sinus bone walls

Table 1 Percentage of new bone and graft remnants within the full elevated area.

Time point	Grafting material	New bone, %			IBN, %		
		Mean ± SD	Median (25%; 75%)	P value	Mean ± SD	Median (25%; 75%)	P value
2 weeks	Bio-Oss	0.7 ± 0.8	0.4 (0.2; 0.6)	0.098	0.0 ± 0.0	0.0 (0.0; 0.0)	NA
	Cerabone	0.3 ± 0.2	0.3 (0.1; 0.4)		0.0 ± 0.1	0.0 (0.0; 0.0)	
10 weeks	Bio-Oss	20.0 ± 4.3	21.4 (18.1; 22.1)	0.041	0.0 ± 0.0	0.0 (0.0; 0.0)	NA
	Cerabone	15.8 ± 4.0	14.5 (13.8; 19.6)		1.3 ± 0.6	1.5 (1.2; 1.5)	

$P < 0.05$.

Table 2 Total bone percentages after 2 weeks of healing. The various regions of the augmented area were evaluated.

Grafting material	Full augmented area			Next-to-window			Central		
	Mean ± SD	Median (25%; 75%)	P value	Mean ± SD	Median (25%; 75%)	P value	Mean ± SD	Median (25%; 75%)	P value
Bio-Oss	0.7 ± 0.8	0.4 (0.2; 0.6)	0.159	0.3 ± 0.5	0.0 (0.0; 0.4)	0.250	0.3 ± 0.8	0.0 (0.0; 0.0)	0.750
Cerabone	0.3 ± 0.3	0.3 (0.1; 0.5)		0.0 ± 0.0	0.0 (0.0; 0.0)		0.1 ± 0.1	0.0 (0.0; 0.0)	

Table 3 Percentage of new bone after 10 weeks of healing. The various regions of the augmented area were assessed.

Grafting material	Full elevated area			Next-to-window			Central		
	Mean ± SD	Median (25%; 75%)	P value	Mean ± SD	Median (25%; 75%)	P value	Mean ± SD	Median (25%; 75%)	P value
Bio-Oss	20.0 ± 4.3	21.4 (18.1; 22.1)	0.162	31.5 ± 8.1	32.4 (28.0; 33.7)	0.018	13.8 ± 8.3	13.4 (7.8; 21.6)	0.585
Cerabone	17.2 ± 4.3	15.8 (14.1; 21.1)		21.9 ± 7.8	22.9 (21.0; 24.6)		12.2 ± 5.1	12.8 (8.6; 15.3)	

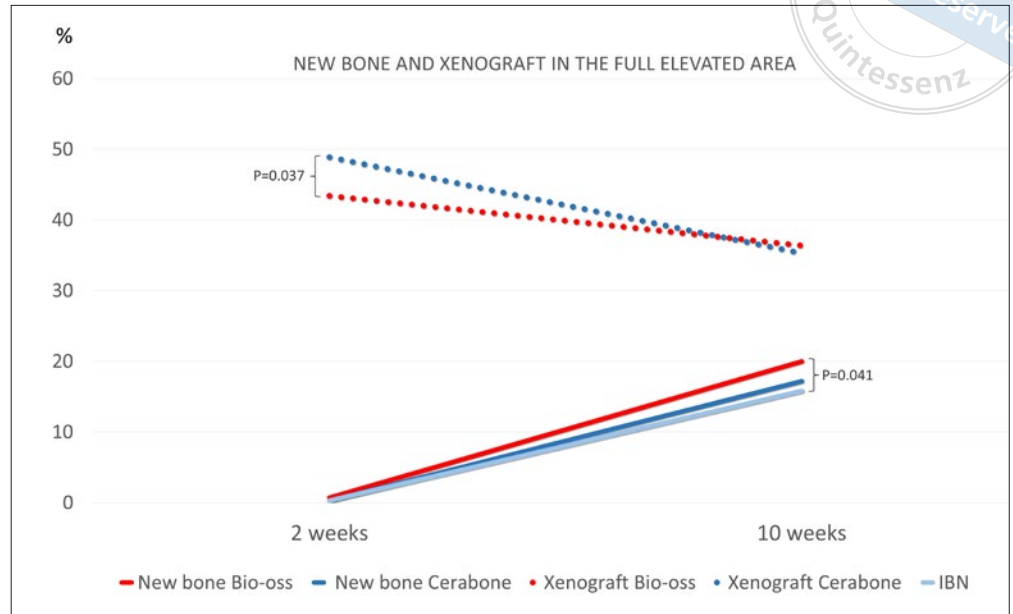


Fig 8 New bone formation and xenogeneic bone graft resorption between 2 and 10 weeks of healing.

(Table 3). In these regions, the total bone percentage was higher in the Bio-Oss group; however, only the difference at the next-to-window wall region was statistically significant ($P = 0.018$). The lowest percentage of new bone was found in the submucosa regions, followed by the central region.

microCT evaluation

The evaluation was performed at two different thresholds of grey levels to identify bone tissue from xenogeneic bone graft, namely 60 to 80 and 70 to 100. After 2 weeks of healing (Figs 9a to c), the tissue vol-

Total bone, %				Residual graft, %		
Mean ± SD	Median (25%; 75%)	P value	Mean ± SD	Median (25%; 75%)	P value	
0.7 ± 0.8	0.4 (0.2; 0.6)	0.159	43.4 ± 6.2	45.6 (40.0; 47.6)	0.037	
0.3 ± 0.3	0.3 (0.1; 0.5)		48.8 ± 4.3	50.0 (49.2; 51.5)		
20.0 ± 4.3	21.4 (18.1; 22.1)	0.162	36.4 ± 4.3	36.4 (35.0; 38.2)	0.846	
17.2 ± 4.3	15.8 (14.1; 21.1)		35.3 ± 10.5	39.7 (33.5; 41.5)		

Submucosa			Lateral wall			Medial wall		
Mean ± SD	Median (25%; 75%)	P value	Mean ± SD	Median (25%; 75%)	P value	Mean ± SD	Median (25%; 75%)	P value
0.0 ± 0.0	0.0 (0.0; 0.0)	1.000	1.0 ± 1.2	0.8 (0.0; 1.3)	0.231	1.7 ± 2.2	0.5 (0.1; 2.6)	0.214
0.0 ± 0.0	0.0 (0.0; 0.0)		0.4 ± 0.5	0.2 (0.0; 0.7)		1.0 ± 1.3	0.3 (0.0; 1.7)	

Submucosa			Lateral wall			Medial wall		
Mean ± SD	Median (25%; 75%)	P value	Mean ± SD	Median (25%; 75%)	P value	Mean ± SD	Median (25%; 75%)	P value
6.9 ± 6.1	5.4 (3.0; 9.6)	0.112	22.1 ± 10.5	21.2 (15.7; 28.6)	0.529	25.7 ± 6.8	27.0 (21.6; 29.1)	0.242
9.7 ± 5.6	11.5 (4.7; 13.6)		19.4 ± 8.5	18.6 (14.8; 25.4)		22.6 ± 8.3	24.3 (18.8; 29.7)	

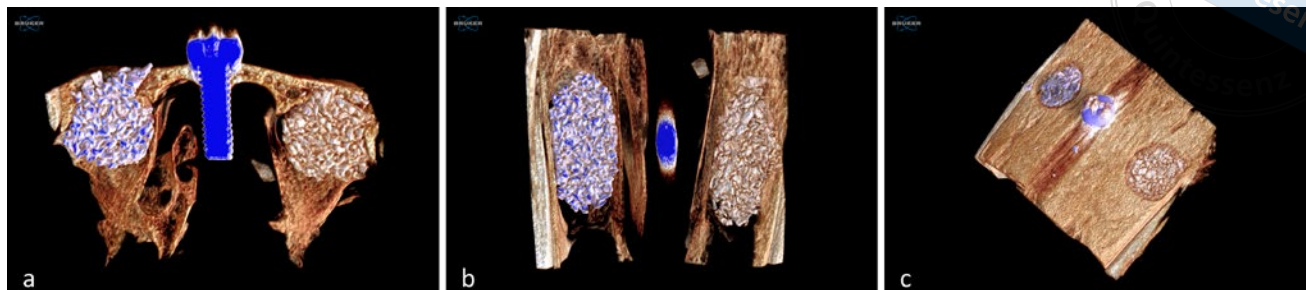


Fig 9 MicroCT 3D images representing healing in the grafted sinus after 2 weeks. **(a)** Coronal; **(b)** from the sinus; **(c)** from the nasal bone. Cerabone grafts are on the left and Bio-Oss grafts are on the right side of the image.

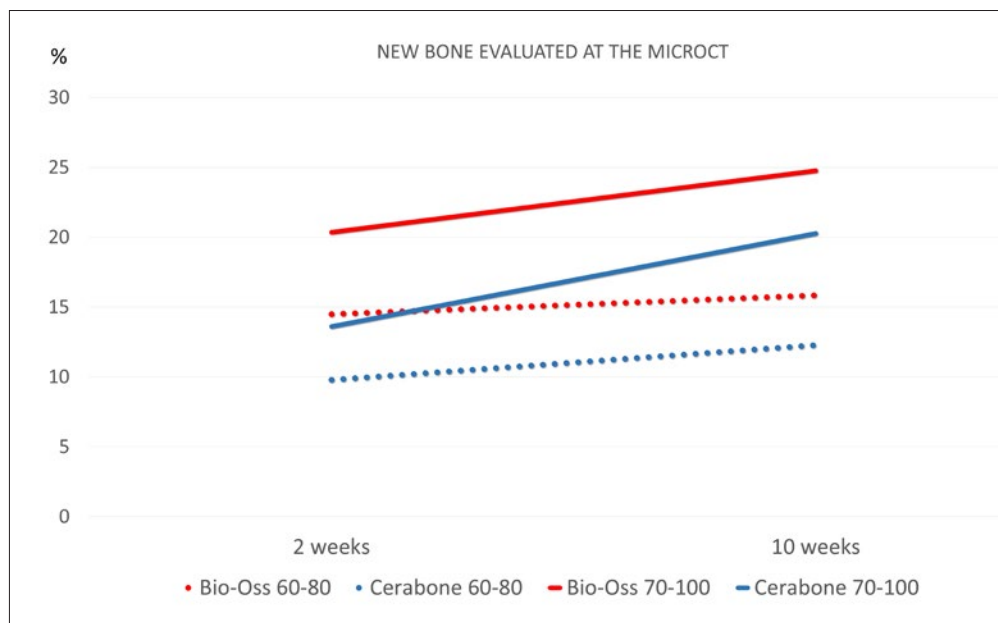


Fig 10 Percentage of new bone evaluated in the microCT analysis using different grey levels: 60 to 80 and 70 to 100.

umes of the elevated spaces were $78.52 \pm 8.89 \text{ mm}^3$ and $80.44 \pm 13.12 \text{ mm}^3$ for the Bio-Oss and Cerabone groups, respectively ($P = 0.208$). The grey level of 60 to 80 yielded $14.48\% \pm 2.29\%$ and $9.79\% \pm 1.27\%$ ($P < 0.0001$) of new bone in the Bio-Oss and Cerabone groups, respectively (Fig 10). Applying a grey level of 70 to 100, the respective proportions of new bone were $20.35\% \pm 3.37\%$ and $13.60\% \pm 2.09\%$ ($P < 0.0001$).

After 10 weeks of healing (Figs 11a to c), the tissue volumes of the elevated spaces were $84.49 \pm 9.78 \text{ mm}^3$ and $92.96 \pm 12.0 \text{ mm}^3$ for the Bio-Oss and Cerabone groups, respectively ($P = 0.057$). The grey level of 60 to 80 disclosed $15.83\% \pm 1.82\%$ and $12.28\% \pm 0.96\%$ ($P < 0.0001$) of new bone in the Bio-Oss and Cerabone groups, respectively. Applying a grey level of 70 to 100, $24.76\% \pm 2.50\%$ was recorded in the Bio-Oss group, and $20.26\% \pm 1.57\%$ in the Cerabone group ($P < 0.0001$).

Correlation between 10-week histological and microCT analyses

Applying a grey level of 60 to 80 for bone tissue evaluation, a weak positive correlation for the Bio-Oss group (0.091 ; $P = 0.811$) and a weak negative correlation for the Cerabone group (-0.333 ; $P = 0.349$) were found. Using a grey level of 70 to 100, a strong positive correlation for the Bio-Oss group (0.709 ; $P = 0.027$) and a weak positive correlation for the Cerabone group (0.212 ; $P = 0.560$) were found.

Discussion

The present study aimed to compare the sequential healing of maxillary sinuses grafted with two different xenogenic bone substitutes sintered at either a low or high temperature. After 10 weeks of healing, the histological

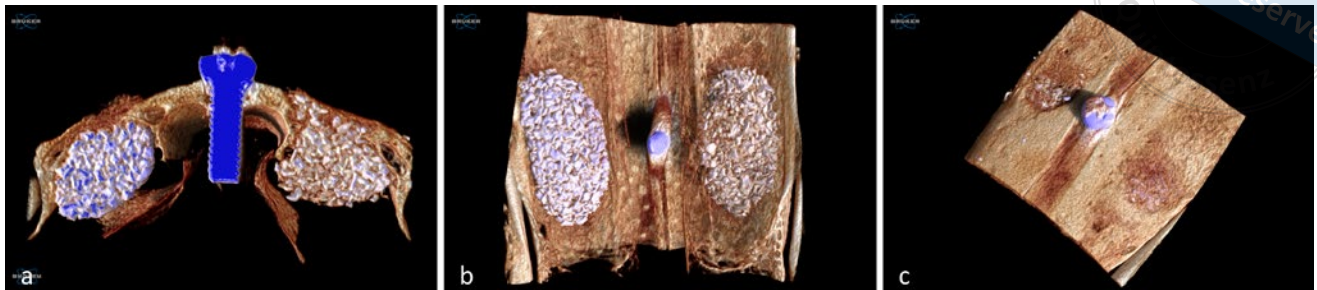


Fig 11 MicroCT 3D images representing healing in the grafted sinus after 10 weeks. **(a)** Coronal; **(b)** from the sinus; **(c)** from the nasal bone. Cerabone grafts are on the left and Bio-Oss grafts are on the right side of the image.

evaluation showed that a tendency towards higher bone formation was found in the Bio-Oss group compared to the Cerabone group; however, the difference was not statistically significant. In both groups, the highest percentages of new bone were observed in the regions close to the bone walls and the osteotomy.

In the Cerabone group, several graft particles presented dark regions with fog-like shadows that hid the hard and soft tissues. These tissues were shown more clearly under the microscope when overexposing the image to the light whereas, when adjusting the focus, no improvement was made in the identification. This method made it possible to identify new bone hidden by the shadows and was illustrated in other articles in which biphasic beta tricalcium phosphate/hydroxyapatite (β -TCP/HA) were used for sinus floor augmentation in sheep⁴⁶ and rabbits⁴⁷ and recently in human biopsy specimens to unveil bone covered by shadows around Cerabone⁴⁸. The total amount of bone reported represented the sum of new bone outside the dark shadows and that covered by those shadows (IBN). The structure of the IBN recalled that of an “interpenetrating polymer network”⁴⁹ and consequently, a similar name was adopted.

After 2 weeks of healing, the percentage of new bone in the full elevated area was < 1% in both groups. The inclusion of an early period of healing in the analysis of the present study enabled the differences in the regions close to the source of new bone to be evaluated and, at the same time, provided the opportunity to assess dimensional variations over time. After 2 weeks of healing, the postsurgical oedema that occurs after sinus floor augmentation⁵⁰⁻⁵³ appeared to be resolved. The resorptive processes were still in an early phase, resulting in little effect on dimensional changes. During this healing period in both groups, bone was formed from the lateral sinus walls while, in the submucosa area, no new bone was found. This is in agreement with several

other reports that showed the absence of participation of the sinus mucosa in bone formation during this early period of healing^{8,9,54-55}.

After 10 weeks, new bone proportions increased in both groups in all regions included in the analyses. In this healing period, the proportion of new bone was 20.0% in the Bio-Oss group and 17.2% in the Cerabone group. A comparison of the results of healing between Bio-Oss and Cerabone after sinus floor augmentation was also performed in a clinical study³¹. Biopsy specimens were harvested after 6 months from the augmented sinus, and the proportion of new bone was 41.4% in the Bio-Oss group and 39.2% in the Cerabone group; however, the difference was not statistically significant³¹. These proportions of new bone were approximately double for both groups compared to the present study. The difference in percentage might be related to the different model used, but also to the fact that the biopsy specimens in the animal study comprised all regions of the sinus, including those with very little bone such as that subjacent to the submucosa. In the previous study, only the region close to the base of the sinus was included in the analysis³¹, i.e., closer to an important source of new bone^{50,51}.

In another clinical study, the analysis performed on biopsy specimens harvested after 8 months from sinus augmentation revealed higher proportions of new bone in the Cerabone group (29.1%) compared to the Bio-Oss group (24.6%)⁵⁶. Again, the difference was not statistically significant.

In the present study, in both groups, the highest amounts of new bone were located close to the bone walls and the osteotomy. Both biomaterials allowed new bone formation and, after 2 weeks, the first signs of incorporation of the neighbouring granules were already noted close to the bone walls. After 10 weeks, incorporation of the granules was observed in all regions. This event has been described in other experimental

studies^{24,27,28}. In an experiment on sinus augmentation in rabbits, the sequential events of bone-to-graft contact at DBBM granules were analysed after 7, 14, 20 and 40 days of healing²⁴. After 7 days, small amounts of bone were found close to the bone walls, whereas the DBBM granules were surrounded by soft tissue containing fibres and fibroblast-like cells arranged in layers in direct contact with the biomaterial surface, and after 14 days, several DBBM granules were covered by newly formed bone; however, the majority were surrounded by dense tissues, similar to those observed after 7 days of healing, and the regions between granules were occupied by loose tissue, poor in cells but rich in vessels²⁴. In the following healing periods, further granules were enclosed by newly formed bone, and the surfaces not covered by bone presented dense tissues²⁴. The regions including those between granules, first occupied by loose tissues, underwent a transformation into primitive bone marrow²⁴.

In the present study, after 10 weeks of healing, new bone in the whole area of the Bio-Oss group reached a proportion of 20.0%. This result is similar to that reported in another study in which Bio-Oss granules were treated with Argon plasma or left untreated before being used to fill the subantral space in rabbits²⁶. The percentages of new bone after 10 weeks were 23.5% in the plasma group and 21.3% in the untreated group. The histological analyses were also performed in the bone wall and central regions of the sinuses²⁶. The proportion of new bone in the group not treated with argon plasma was 26.3% in the bone wall region, and 13.2% in the central regions²⁶. These data are consistent with those of the present study, with the proportion of new bone being approximately 22.0% to 26.0% in the bone wall region and 13.8% in the central region.

In both groups in the present study, the submucosa region exhibited lower amounts of new bone compared to the other regions examined, namely 6.9% and 9.7% in the Bio-Oss and Cerabone groups, respectively. Other similar experiments on sinus augmentation in rabbits reported data on bone formation in this region⁵⁷⁻⁶¹. The presence of new bone subjacent to the sinus mucosa cannot exclude its contribution to bone formation; however, if this contribution does exist, it is limited. It is also necessary to consider that several perforations of the sinus mucosa were observed with relation to the biomaterial particles in both groups. It has been shown in a rabbit model that the presence of sinus mucosa perforations compromised new bone formation in the adjacent regions within the sinus⁶².

The difference in percentage between 2 and 10 weeks of healing was 7.0% for Bio-Oss and 13.5% for

Cerabone. This means that part of the biomaterial was resorbed or lost through the osteotomy or the sinus mucosa. Indeed, several osteoclastic-like zones were observed around both biomaterials at the 2-week evaluation period whereas after 10 weeks, osteoclastic-like cells were rarely observed. This observation agrees with other reports that showed a progressively decreasing percentage of osteoclasts within the augmented space over time^{54,55}.

The two bovine cancellous bone grafts used in the present experiment as fillers for sinus augmentation were processed at different temperatures, namely 300°C for Bio-Oss and 1200°C for Cerabone. The process carried out at a high temperature produces macroporous particles with increased crystallinity which might result in slower resorption of the graft, and decreases the microporosity of the surface which might also reduce the osteoconductivity⁶³⁻⁶⁵. In the present study, however, despite the use of similar volumes of biomaterial in all sinuses, slightly higher volumes were found after 10 weeks compared to 2 weeks of healing. This in turn means that the volumes were maintained over time or even increased, perhaps for bone apposition.

The microCT showed higher percentages of new bone in the Bio-Oss group compared to the Cerabone group ($P > 0.0001$). The data yielded from the microCT analysis were not completely in agreement with those from the histological analysis, especially for the 2-week period. These differences might be ascribed to the fact that histology is a 2-dimensional analysis that represents only a central, limited portion of the sinus that includes the osteotomy. The microCT analysis instead assesses the whole volume that also includes regions located distally and mesially to the osteotomy, in contact with the nasal bone, that represent a further source for bone formation; however, another aspect that should be considered is that the microCT analysis might make it difficult to discriminate between bone and xenogeneic bone graft, yielding contradictory outcomes compared to the histological assessments, especially in the earliest periods of healing^{25,66}. Indeed, three out of four correlations evaluated between the bone percentage after 10 weeks in the Bio-Oss and Cerabone groups were weak, whereas only that for the Bio-Oss group applying a grey level of 70 to 100 was strong positive.

With regard to the limitations of the present study, the dark fog-like shadows present in some regions of Cerabone granules should be mentioned. This event, perhaps due to the high porosity of the biomaterial, the stain characteristics or the slow degradation of the biomaterial⁶⁷, might obstruct identification of new bone and decrease the percentage of new bone detected with

Cerabone. The model used represents another limitation of the study considering the dimensions of the sinus and the lower thickness of the sinus mucosa compared to humans⁵⁴. Moreover, healing in rabbits has been shown to be faster compared to humans⁶⁸; thus, any inferences about humans must be taken with caution.

Conclusion

The present study illustrated that both biomaterials provided conditions that allowed bone growth within the elevated space and confirmed that both biomaterials are suitable to be used as graft materials for sinus floor augmentation. The overexposure to the microscope light in the histological preparation might help to identify the tissues veiled by the dark shadows surrounding Cerabone particles.

Acknowledgements

The authors acknowledge the contribution of Sebastião Bianco (Faculty of Dentistry of Ribeirão Preto, São Paulo, Brazil) for the histological processing. The Cerabone xenogeneic bone graft was provided free of charge by Straumann Italy, Milan, Italy.

Conflicts of interest

The authors declare no conflicts of interest related to this study.

Author contribution

Drs Vitor FERREIRA BALAN, Daniele BOTTICELLI, David PEÑARROCHA-OLTRA and Samuel Porfirio XAVIER contributed to the conceptualization of the study; Vitor FERREIRA BALAN and Eduardo PIRES GODOY contributed to surgical procedures; Dr Vitor FERREIRA BALAN contributed to the histological and microCT analyses; Drs Vitor FERREIRA BALAN, Daniele BOTTICELLI and Katsuhiko MASUDA contributed to the data analysis; Drs Daniele BOTTICELLI and Samuel Porfirio XAVIER contributed to the supervision of the project; Drs Vitor FERREIRA BALAN and Daniele BOTTICELLI contributed to the manuscript draft; Drs David PEÑARROCHA-OLTRA, Katsuhiko MASUDA, Daniele BOTTICELLI and Samuel Porfirio XAVIER contributed to finalising the article. All authors have read and approved the published version of the manuscript.

(Received Jan 30, 2022; accepted Mar 09, 2022)

References

1. Pjetursson BE, Tan WC, Zwahlen M, Lang NP. A systematic review of the success of sinus floor elevation and survival of implants inserted in combination with sinus floor elevation. *J Clin Periodontol* 2008;35(8, suppl):216–240.
2. Asai S, Shimizu Y, Ooya K. Maxillary sinus augmentation model in rabbits: Effect of occluded nasal ostium on new bone formation. *Clin Oral Implants Res* 2002;13:405–409.
3. Xu H, Shimizu Y, Asai S, Ooya K. Grafting of deproteinized bone particles inhibits bone resorption after maxillary sinus floor elevation. *Clin Oral Implants Res* 2004;15:126–133.
4. Corbella S, Taschieri S, Weinstein R, Del Fabbro M. Histomorphometric outcomes after lateral sinus floor elevation procedure: a systematic review of the literature and meta-analysis. *Clin Oral Implants Res* 2016;27:1106–1122.
5. Ellegaard B, Kølsen-Petersen J, Baelum V. Implant therapy involving maxillary sinus lift in periodontally compromised patients. *Clin Oral Implants Res* 1997;8:305–315.
6. Lundgren S, Andersson S, Gualini F, Sennerby L. Bone reformation with sinus membrane elevation: A new surgical technique for maxillary sinus floor augmentation. *Clin Implant Dent Relat Res* 2004;6:165–173.
7. Ellegaard B, Baelum V, Kølsen-Petersen J. Non-grafted sinus implants in periodontally compromised patients: A time-to-event analysis. *Clin Oral Implants Res* 2006;17:156–164.
8. Scala A, Botticelli D, Faeda RS, Rangel IG Jr, de Oliveira JA, Lang NP. Lack of influence of the Schneiderian membrane in forming new bone apical to implants simultaneously installed with sinus floor elevation: An experimental study in monkeys. *Clin Oral Implants Res* 2012;23:175–181.
9. Scala A, Botticelli D, Rangel IG Jr, de Oliveira JA, Okamoto R, Lang NP. Early healing after elevation of the maxillary sinus floor applying a lateral access: A histological study in monkeys. *Clin Oral Implants Res* 2010;21:1320–1326.
10. Cricchio G, Palma VC, Faria PE, et al. Histological findings following the use of a space-making device for bone reformation and implant integration in the maxillary sinus of primates. *Clin Implant Dent Relat Res* 2009;11(suppl 1):e14–e22.
11. Cricchio G, Palma VC, Faria PE, et al. Histological outcomes on the development of new space-making devices for maxillary sinus floor augmentation. *Clin Implant Dent Relat Res* 2011;13:224–230.
12. Schweikert M, Botticelli D, de Oliveira JA, Scala A, Salata LA, Lang NP. Use of a titanium device in lateral sinus floor elevation: An experimental study in monkeys. *Clin Oral Implants Res* 2012;23:100–105.
13. Johansson LÅ, Isaksson S, Adolfsson E, Lindh C, Sennerby L. Bone regeneration using a hollow hydroxyapatite space-maintaining device for maxillary sinus floor augmentation--A clinical pilot study. *Clin Implant Dent Relat Res* 2012;14:575–584.
14. Klijjn RJ, Meijer GJ, Bronkhorst EM, Jansen JA. Sinus floor augmentation surgery using autologous bone grafts from various donor sites: A meta-analysis of the total bone volume. *Tissue Eng Part B Rev* 2010;16:295–303.
15. De Santis E, Lang NP, Ferreira S, Garcia IR Jr, Caneva M, Botticelli D. Healing at implants installed concurrently to maxillary sinus floor elevation with Bio-Oss® or autologous bone grafts. A histomorphometric study in rabbits. *Clin Oral Implants Res* 2017;28:503–511.
16. Scala A, Lang NP, de Carvalho Cardoso L, Pantani F, Schweikert M, Botticelli D. Sequential healing of the elevated sinus floor after applying autologous bone grafting: An experimental study in minipigs. *Clin Oral Implants Res* 2015;26:419–425.
17. Clavero J, Lundgren S. Ramus or chin grafts for maxillary sinus inlay and local onlay augmentation: Comparison of donor site morbidity and complications. *Clin Implant Dent Relat Res* 2003;5:154–160.

18. Jensen T, Schou S, Svendsen PA, et al. Volumetric changes of the graft after maxillary sinus floor augmentation with Bio-Oss and autogenous bone in different ratios: A radiographic study in minipigs. *Clin Oral Implants Res* 2012;23:902–910.
19. Sbordone L, Levin L, Guidetti F, Sbordone C, Glikman A, Schwartz-Arad D. Apical and marginal bone alterations around implants in maxillary sinus augmentation grafted with autogenous bone or bovine bone material and simultaneous or delayed dental implant positioning. *Clin Oral Implants Res* 2011;22:485–491.
20. Jensen T, Schou S, Stavropoulos A, Terheyden H, Holmstrup P. Maxillary sinus floor augmentation with Bio-Oss or Bio-Oss mixed with autogenous bone as graft in animals: A systematic review. *Int J Oral Maxillofac Surg* 2012;41:114–120.
21. Manfro R, Fonseca FS, Bortoluzzi MC, Sendyk WR. Comparative, histological and histomorphometric analysis of three anorganic bovine xenogenous bone substitutes: Bio-Oss, Bone-Fill and Gen-Ox Anorganic. *J Maxillofac Oral Surg* 2014;13:464–470.
22. Moon JW, Sohn DS, Heo JU, Kim JS. Comparison of two kinds of bovine bone in maxillary sinus augmentation: A histomorphometric study. *Implant Dent* 2015;24:19–24.
23. Mordenfeld A, Lindgren C, Hallman M. Sinus floor augmentation using Straumann® BoneCeramic™ and Bio-Oss® in a split mouth design and later placement of implants: A 5-year report from a longitudinal study. *Clin Implant Dent Relat Res* 2016;18:926–936.
24. Caneva M, Lang NP, Rangel IG Jr, et al. Sinus mucosa elevation using Bio-Oss® or Gingistat® collagen sponge: an experimental study in rabbits. *Clin Oral Implants Res* 2017;28:e21–e30.
25. Iida T, Baba S, Botticelli D, Masuda K, Xavier SP. Comparison of histomorphometry and microCT after sinus augmentation using xenografts of different particle sizes in rabbits. *Oral Maxillofac Surg* 2020;24:57–64.
26. Hirota A, Yamada Y, Canullo L, Xavier SP, Baba S. Bioactivation of bovine bone matrix using argon plasma: An experimental study for sinus augmentation in rabbits. *Int J Oral Maxillofac Implants* 2020;35:731–738.
27. Busenlechner D, Huber CD, Vasak C, Dobsak A, Gruber R, Watzek G. Sinus augmentation analysis revised: The gradient of graft consolidation. *Clin Oral Implants Res* 2009;20:1078–1083.
28. Godoy EP, Alccayhuaman KAA, Botticelli D, et al. Osteoconductivity of bovine xenograft granules of different sizes in sinus lift: A histomorphometric study in rabbits. *Dent J (Basel)* 2021;9:61.
29. Galindo-Moreno P, Hernández-Cortés P, Aneiros-Fernández J, et al. Morphological evidences of Bio-Oss® colonization by CD44-positive cells. *Clin Oral Implants Res* 2014;25:366–371.
30. Riachi F, Naaman N, Tabarani C, et al. Influence of material properties on rate of resorption of two bone graft materials after sinus lift using radiographic assessment. *Int J Dent* 2012;2012:737262.
31. Mahesh L, Mascarenhas G, Bhasin MT, Guirado C, Juneja S. Histological evaluation of two different anorganic bovine bone matrixes in lateral wall sinus elevation procedure: A retrospective study. *Natl J Maxillofac Surg* 2020;11:258–262.
32. Zahedpasha A, Ghassemi A, Bijani A, Haghaniifar S, Majidi MS, Ghorbani ZM. Comparison of bone formation after sinus membrane lifting without graft or using bone substitute “histologic and radiographic evaluation”. *J Oral Maxillofac Surg* 2021;79:1246–1254.
33. Tawil G, Barbeck M, Unger R, Tawil P, Witte F. Sinus floor elevation using the lateral approach and window repositioning and a xenogeneic bone substitute as a grafting material: A histologic, histomorphometric, and radiographic analysis. *Int J Oral Maxillofac Implants* 2018;33:1089–1096.
34. Imai H, Lang NP, Ferri M, Hirota A, Apaza Alccayhuaman KA, Botticelli D. Tomographic assessment on the influence of the use of a collagen membrane on dimensional variations to protect the antrostomy after maxillary sinus floor augmentation: A randomized clinical trial. *Int J Oral Maxillofac Implants* 2020;35:350–356.
35. Perić Kačarević Z, Kavehei F, Houshmand A, et al. Purification processes of xenogeneic bone substitutes and their impact on tissue reactions and regeneration. *Int J Artif Organs* 2018;41:789–800.
36. Laschke MW, Witt K, Pohlemann T, Menger MD. Injectable nanocrystalline hydroxyapatite paste for bone substitution: In vivo analysis of biocompatibility and vascularization. *J Biomed Mater Res B Appl Biomater* 2007;82:494–505.
37. Huber FX, Berger I, McArthur N, et al. Evaluation of a novel nanocrystalline hydroxyapatite paste and a solid hydroxyapatite ceramic for the treatment of critical size bone defects (CSD) in rabbits. *J Mater Sci Mater Med* 2008;19:33–38.
38. Catros S, Sandgren R, Pippenger BE, Fricain JC, Herber V, El Char E. A novel xenograft bone substitute supports stable bone formation in circumferential defects around dental implants in minipigs. *Int J Oral Maxillofac Implants* 2020;35:1122–1131.
39. Shakir M, Jolly R, Khan AA, et al. Resol based chitosan/nano-hydroxyapatite nanoensemble for effective bone tissue engineering. *Carbohydr Polym* 2018;179:317–327.
40. Kumlien J, Schiratzki H. Blood flow in the rabbit sinus mucosa during experimentally induced chronic sinusitis. Measurement with a diffusible and with a non-diffusible tracer. *Acta Otolaryngol* 1985;99:630–636.
41. Kennedy DW, Shaalan H. Reevaluation of maxillary sinus surgery: Experimental study in rabbits. *Ann Otol Rhinol Laryngol* 1989;98:901–906.
42. Trajkovski B, Jaunich M, Müller WD, Beuer F, Zafiroopoulos GG, Houshmand A. Hydrophilicity, viscoelastic, and physicochemical properties variations in dental bone grafting substitutes. *Materials (Basel)* 2018;11:215.
43. Costa MM, Botticelli D, Moses O, et al. Maxillary sinus augmentation using ceramic alloplastic granules or paste: An experimental study in rabbits. *Dent J (Basel)* 2021;9:65.
44. Lee JH, Yi GS, Lee JW, Kim DJ. Physicochemical characterization of porcine bone-derived grafting material and comparison with bovine xenografts for dental applications. *J Periodontal Implant Sci* 2017;47:388–401.
45. Schroeder HE, Münzel-Pedrazzoli S. Correlated morphometric and biochemical analysis of gingival tissue. Morphometric model, tissue sampling and test of stereologic procedures. *J Microsc* 1973;99:301–329.
46. Perini A, Ferrante G, Sivolella S, Velez JU, Bengazi F, Botticelli D. Bone plate repositioned over the antrostomy after sinus floor elevation: An experimental study in sheep. *Int J Implant Dent* 2020;6:11.
47. Tanaka K, Botticelli D, Canullo L, Baba S, Xavier SP. New bone ingrowth into β -TCP/HA graft activated with argon plasma: A histomorphometric study on sinus lifting in rabbits. *Int J Implant Dent* 2020;6:36.
48. Kotsu M, Apaza Alccayhuaman KA, Ferri M, et al. Osseointegration at implants installed in composite bone. A histological randomized clinical trial on sinus floor elevation. *J Funct Biomater* 2022;13:22.
49. International Union of Pure and Applied Chemistry. Compendium of Chemical Terminology (the “Gold Book”), ed 2. <https://goldbook.iupac.org/> Accessed April 30 2022.
50. Kawakami S, Lang NP, Iida T, Ferri M, Apaza Alccayhuaman KA, Botticelli D. Influence of the position of the antrostomy in sinus floor elevation assessed with cone-beam computed tomography: A randomized clinical trial. *J Investig Clin Dent* 2018;9:e12362.
51. Kawakami S, Lang NP, Ferri M, Apaza Alccayhuaman KA, Botticelli D. Influence of the height of the antrostomy in sinus floor elevation assessed by cone beam computed tomography – A randomized clinical trial. *Int J Oral Maxillofac Implants* 2019;34:223–232.
52. Kato S, Omori Y, Kanayama M, et al. Sinus mucosa thickness changes and ostium involvement after maxillary sinus floor elevation in sinus with septa. A cone beam computed tomography study. *Dent J (Basel)* 2021;9:82.
53. Sakuma S, Ferri M, Imai H, et al. Involvement of the maxillary sinus ostium (MSO) in the edematous processes after sinus floor augmentation: a cone-beam computed tomographic study. *Int J Implant Dent* 2020;6:35.

54. Iida T, Carneiro Martins Neto E, Botticelli D, Apaza Alccayhuaman KA, Lang NP, Xavier SP. Influence of a collagen membrane positioned subjacent the sinus mucosa following the elevation of the maxillary sinus. A histomorphometric study in rabbits. *Clin Oral Implants Res* 2017;28:1567–1576.
55. Omori Y, Ricardo Silva E, Botticelli D, Apaza Alccayhuaman KA, Lang NP, Xavier SP. Reposition of the bone plate over the antrotomy in maxillary sinus augmentation: A histomorphometric study in rabbits. *Clin Oral Implants Res* 2018;29:821–834.
56. Panagiotou D, Özkan Karaca E, Dirikan İpçi Ş, Çakar G, Olgaç V, Yılmaz S. Comparison of two different xenografts in bilateral sinus augmentation: Radiographic and histologic findings. *Quintessence Int* 2015;46:611–619.
57. Amari Y, Botticelli D, Apaza Alccayhuaman KA, Hirota A, Silva ER, Xavier SP. The influence on healing of bony window elevated inward in the sinus cavity as cortical bone graft: A histomorphometric study in rabbit model. *Int J Oral Maxillofac Implants* 2020;35:879–887.
58. Masuda K, Silva ER, Botticelli D, Apaza Alccayhuaman KA, Xavier SP. Antrotomy preparation for maxillary sinus floor augmentation using drills or a sonic instrument: A microcomputed tomography and histomorphometric study in rabbits. *Int J Oral Maxillofac Implants* 2019;34:819–827.
59. Scala A, Viña-Almunia J, Carda C, et al. Sequential healing of the elevated sinus floor with different size of antrotomy: A histomorphometric study in rabbits. *Oral Maxillofac Surg* 2020;24:403–410.
60. Scala A, Lang NP, Urbizo Velez J, Favero R, Bengazi F, Botticelli D. Effects of a collagen membrane positioned between augmentation material and the sinus mucosa in the elevation of the maxillary sinus floor. An experimental study in sheep. *Clin Oral Implants Res* 2016;27:1454–1461.
61. Favero V, Lang NP, Canullo L, Urbizo Velez J, Bengazi F, Botticelli D. Sinus floor elevation outcomes following perforation of the Schneiderian membrane. An experimental study in sheep. *Clin Oral Implants Res* 2016;27:233–240.
62. Paik JW, Cha JK, Song YW, Thoma DS, Jung RE, Jung UW. Effect of Schneiderian membrane integrity on bone formation in sinus augmentation: An experimental study in rabbits. *J Clin Periodontol* 2022;49:76–83.
63. Block MS. Does the use of high-temperature-processed xenografts for ridge augmentation result in ridge width stability over time? *J Oral Maxillofac Surg* 2020;78:1717–1725.
64. Block MS. The processing of xenografts will result in different clinical responses. *J Oral Maxillofac Surg* 2019;77:690–697.
65. Ramírez Fernández MP, Mazón P, Gehrke SA, Calvo-Guirado JL, De Aza PN. Comparison of two xenograft materials used in sinus lift procedures: Material characterization and in vivo behavior. *Materials (Basel)* 2017;10:623.
66. Iida T, Silva ER, Lang NP, Apaza Alccayhuaman KA, Botticelli D, Xavier SP. Histological and micro-computed tomography evaluations of newly formed bone after maxillary sinus augmentation using a xenograft with similar density and mineral content of bone: An experimental study in rabbits. *Clin Exp Dent Res* 2018;4:284–290.
67. Iezzi G, Piattelli A, Giuliani A, et al. Molecular, cellular and pharmaceutical aspects of bone grafting materials and membranes during maxillary sinus-lift procedures. Part 2: Detailed characteristics of the materials. *Curr Pharm Biotechnol* 2017;18:33–44.
68. Botticelli D, Lang NP. Dynamics of osseointegration in various human and animal models – A comparative analysis. *Clin Oral Implants Res* 2017;28:742–748.